JOURNAL OF BACTERIOLOGY, Aug. 1995, p. 4721–4729 Vol. 177, No. 16
0021-9193/95/$04.00+0

The *Bacillus subtilis dacB* Gene, Encoding Penicillin-Binding Protein 5*, Is Part of a Three-Gene Operon Required for Proper Spore Cortex Synthesis and Spore Core Dehydration

DAVID L. POPHAM, BERENICE ILLADES-AGUIAR, AND PETER SETLOW*

Department of Biochemistry, University of Connecticut Health Center, Farmington, Connecticut 06030-3305

Received 10 April 1995/Accepted 8 June 1995

Studies of gene expression using fusions to *lacZ* demonstrated that the *Bacillus subtilis dacB* gene, encoding penicillin-binding protein 5*, is in an operon with two downstream genes, *spmA* and *spmB*. Mutations affecting any one of these three genes resulted in the production of spores with reduced heat resistance. The cortex peptidoglycan in *dacB* mutant spores had more peptide side chains, a higher degree of peptide cross-linking, and possibly less muramic acid lactam than that of wild-type spores. These cortex structure parameters were normal in *spmA* and *spmB* mutant spores, but these spores did not attain normal spore core dehydration. This defect in spore core dehydration was exaggerated by the additional loss of *dacB* expression. However, loss of *dacB* alone did not alter the spore core water content. Spores produced by *spmA* and *spmB* mutants germinated faster than did those of the wild type. Spores produced by *dacB* mutants germinated normally but were delayed in spore outgrowth. Electron microscopy revealed a drastically altered appearance of the cortex in *dacB* mutants and a minor alteration in an *spmA* mutant. Measurements of electron micrographs indicate that the ratio of the spore protoplast volume to the sporoplast (protoplast-plus-cortex) volume was increased in *dacB* and *spmA* mutants. These results are consistent with spore core water content being the major determinant of spore heat resistance. The idea that loosely cross-linked, flexible cortex peptidoglycan has a mechanical activity involved in achieving spore core dehydration is not consistent with normal core dehydration in spores lacking only *dacB*.

Bacteria of the *Bacillus*, *Clostridium*, and some related genera form dormant endospores which are resistant to a variety of physical and chemical treatments. A number of characteristics of the spore core or protoplast affect the degree of heat resistance. These include the water content (5, 29), the identity of the cations in the spore associated with dipicolinic acid (DPA) (reviewed in reference 12), and the presence of α/β-type, small, acid-soluble proteins (SASP) associated with the chromosomal DNA (28). We have become particularly interested in the correlation of heat resistance with the water content of the spore core, a correlation which has been demonstrated across a variety of species, with spores prepared at different temperatures, and with spores containing different cations (5, 29), as well as in the mechanism by which the water content of the spore core is reduced.

In addition to a correlation with heat resistance, spore core dehydration appears to be required for processing of a spore germination protease, GPR, from its zymogen form to an active form late in sporulation (17, 36). The reduced level of spore core water is theorized to be the factor which prevents degradation of SASP by GPR during late sporulation, since this degradation normally takes place only during spore germination.

The integrity and amount of the spore cortex, a thick peptidoglycan structure which surrounds the spore core, have been shown to be important for maintenance of heat resistance (18, 21; reviewed in reference 12), and degradation of the cortex, by artificial means or during spore germination, results in rapid rehydration of the spore core. These observations indicate that the cortex serves as a retaining structure to withstand the turgor pressure generated by the high concentration of solutes in the spore core. The major modification of the cortex peptidoglycan with respect to the vegetative wall peptidoglycan is the absence of a peptide side chain on ~50% of the muramic acid residues and conversion of these residues to muramic acid lactam (46, 47). The role that this modification plays in cortex function, if any, is unknown, but the lack of peptide side chains on these muramic acid residues limits the degree of peptide-peptide cross-linking that can take place. Peptidoglycan expands and contracts in response to changes in the pH and ionic conditions of its environment (31). The degree of peptide cross-linking is one factor determining the amount of peptidoglycan flexibility, with loosely cross-linked peptidoglycan exhibiting the greatest flexibility (31). This observation is consistent with proposals that the cortex may have a role in bringing about spore core dehydration via a mechanical activity. Prevailing theories suggest that in response to some change in its environment, the cortex contracts (25) or expands anisotropically (45) to reduce the volume of the spore core and effectively expel water. Demonstrations that the cortex peptidoglycan is loosely cross-linked (33, 47) are consistent with these processes taking place.

Further study of cortex synthesis may shed light on the role the cortex plays in attaining and maintaining spore dehydration. Peptidoglycan synthesis is carried out by members of the penicillin-binding protein (PBP) family (13). One member of this protein family, PBP5*, was identified as a PBP expressed only during sporulation slightly prior to the initiation of cortex

* Corresponding author. Phone: (203) 679-2607. Fax: (203) 679-3408. Electronic mail address: Setlow@panda.uchc.edu.

TABLE 1. *B. subtilis* strains used

Strain	Genotype or phenotype[a]	Donor[b]	Recipient[b]	Source or reference
CB11	*dacB*$^+$::Cm^r *trpC2*	pCB1	168	C. Buchanan (10)
CB36	*dacB*::Cm^r *trpC2*	pCB3	168	C. Buchanan (9)
PS832	Prototrophic revertant of 168			Lab stock
PS1669	pPS1669 Kn^r (high GPR expression)	pPS1669	PS832	41
PS1899	*dacB*::Cm^r	CB36	PS832	
PS2029	*spmB*::Cm^r	pDPC215	PS832	
PS2030	*spmA*::Cm^r	pDPC219	PS832	
PS2065	Two copies of in-frame Δ*dacB* Cm^r	pDPC221	PS832	
PS2066	In-frame Δ*dacB* Cm^s			PS2065 exigrant
PS2164	Two copies of in-frame Δ*spmA* Cm^r	pDPC226	PS832	
PS2185	In-frame Δ*spmA* Cm^s			PS2164 exigrant
PS2198	*dacB*::Cm^r pPS1669 Kn^r (high GPR expression)	pPS1669	PS832	
PS2215	*spmA-lacZ*[c] Sp^r	pDPC227[d]	PS832	
PS2216	*dacB-lacZ*[c] Sp^r	pDPC229[d]	PS832	
PS2217	*spmB-lacZ*[c] Sp^r	pDPC230[d]	PS832	
PS2221	*dacB*::Cm^r *spmA-lacZ*[c] Sp^r	PS2215	PS1899	
PS2222	*dacB*::Cm^r *spmB-lacZ*[c] Sp^r	PS2217	PS1899	
PS2224	In-frame Δ*dacB spmA-lacZ*[c] Sp^r	pDPC227[d]	PS2066	
PS2225	In-frame Δ*dacB spmB-lacZ*[c] Sp^r	pDPC230[d]	PS2066	
PS2232	In-frame Δ*spmA spmB-lacZ*[c] Sp^r	pDPC230[d]	PS2185	
PS2239	*spmA-lacZ*[e] Sp^r	pDPC234[d]	PS832	
PS2240	*dacB-lacZ*[e] Sp^r	pDPC235[d]	PS832	
PS2241	*spmB-lacZ*[e] Sp^r	pDPC236[d]	PS832	
PS2242	In-frame Δ*dacB spmA-lacZ*[e] Sp^r	pDPC234[d]	PS2066	
PS2243	In-frame Δ*dacB spmB-lacZ*[e] Sp^r	pDPC236[d]	PS2066	
PS2244	In-frame Δ*spmA spmB-lacZ*[e] Sp^r	pDPC236[d]	PS2185	
PS2245	*dacB*::Cm^r *spmA-lacZ*[e] Sp^r	PS2239	PS1899	
PS2246	*dacB*::Cm^r *spmB-lacZ*[e] Sp^r	PS2241	PS1899	
PS2260	In-frame Δ*dacB* pPS1669 Kn^r (high GPR expression)	pPS1669	PS2066	
PS2261	In-frame Δ*spmA* pPS1669 Kn^r (high GPR expression)	pPS1669	PS2185	

[a] Abbreviation: Kn^r, kanamycin resistance.
[b] Role in transformation.
[c] Translational fusion to *lacZ*.
[d] Construction was accomplished by transformation with the indicated plasmid followed by transformation with linear pJL62 (27) to convert Cm^r to Sp^r.
[e] Transcriptional fusion to *lacZ*.

synthesis (41, 44). An insertion mutation in *dacB*, the gene encoding PBP5*, resulted in the production of spores with significantly reduced heat resistance (9). Further sequencing of the chromosome in the region of *dacB* has revealed that this may be the first gene in a three-gene operon (39). This raised the possibility that the effect of the original *dacB* insertion mutation on heat resistance might have been due to a polar effect on expression of a downstream gene. We demonstrate here that *dacB* is indeed in an operon structure and also present data on the effects of mutations affecting the three genes of this operon individually on spore heat resistance, spore core dehydration, and cortex structure. We have also examined the effects of increased spore core water content on processing of GPR to its active form and on the ability of GPR to degrade SASP in a more-hydrated environment.

MATERIALS AND METHODS

Bacterial strains, growth, and purification of spores. All *Bacillus subtilis* strains described in Table 1 were derivatives of strain 168. *B. subtilis* was transformed as described previously (1). Growth for sporulation and studies of gene expression was in 2× SG medium (24) at 37°C. Spore chloroform resistance was assayed as described previously (30). Spores were purified by water washing as described previously (30). Spore heat resistance was determined by measuring the number of CFU in a spore suspension before and after heating. The D_{90} of a spore preparation is defined as the time at 90°C required to reduce spore viability by 90%. Germination was carried out at 37°C in 2× YT medium (16 g of tryptone, 10 g of yeast extract, and 5 g of NaCl per liter) containing 4 mM L-alanine. In some experiments, spores were heat activated at 70°C for 15 min prior to germination.

Mutant strain constructions. Plasmid pCB1 (10) (Fig. 1) was recovered by digesting chromosomal DNA from strain CB11 (10) with *Hin*dIII, ligating it, and transforming *Escherichia coli* with selection for ampicillin resistance. Production of circular pCB1 by this procedure presumably resulted from a duplication of the plasmid in the chromosome. DNA containing the genes downstream of *dacB* was isolated by digesting the chromosomal DNA of strain PS1899 with *Hin*dIII, ligating it, and transforming *E. coli* with selection for ampicillin resistance. This procedure produced pDPC211 (Fig. 1), which contains 1.7 kb of DNA downstream of the original insert found in pCB3 (9) (Fig. 1).

The 244-bp *Eco*RI-*Rsa*I fragment of pDPC211 was inserted into *Eco*RI-

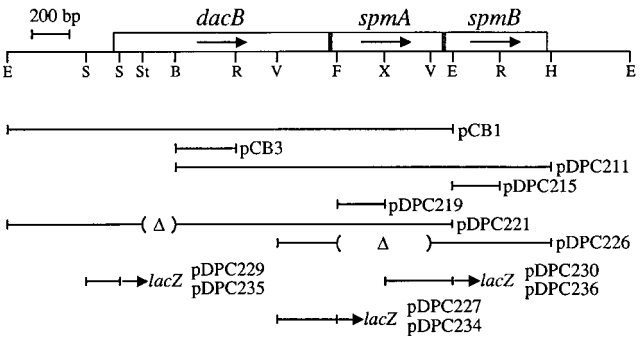

FIG. 1. Map of the *dacB* locus and plasmid constructs. Open reading frames are represented by open boxes. Arrows within the boxes represent the directions of transcription. Restriction endonuclease cleavage site abbreviations: B, *Bgl*II; E, *Eco*RI; F, *Hin*fI; H, *Hin*dIII; R, *Rsa*I; S, *Sau*3AI; St, *Sty*I; V, *Eco*RV; X, *Xmn*I. Only those *Hin*fI, *Sau*3AI, and *Rsa*I sites used in plasmid constructions are shown. Bars below the map represent the inserts in the indicated plasmids. The gaps and Δ symbols in pDPC221 and pDPC226 represent in-frame deletions of *dacB* and *spmA*, respectively. Arrows pointing to *lacZ* indicate the direction of transcription in *lacZ* fusion constructs.

*Hin*cII-digested pUC19 to produce pDPC218. The small *Eco*RI-*Hin*dIII fragment of pDPC218 was inserted into *Eco*RI-*Hin*dIII-digested pJH101 to produce pDPC215 (Fig. 1). The 1,117-bp *Bgl*II-*Xmn*I fragment from pCB1 was inserted into *Bam*HI-*Hin*cII-digested pUC19 to produce pDPC214. This plasmid was digested with *Hin*fI, treated with the Klenow fragment of *E. coli* DNA polymerase I and deoxynucleoside triphosphates (dNTPs) to render the ends blunt, and finally digested with *Hin*dIII. The resulting 285-bp fragment was inserted into *Hin*dIII-*Hin*cII-digested pUC19 to produce pDPC217. The 335-bp *Eco*RI-*Hin*dIII fragment of pDPC217 was inserted into *Eco*RI-*Hin*dIII-digested pJH101 to produce pDPC219 (Fig. 1). The plasmids pDPC215 and pDPC219 were transformed into *B. subtilis* with selection for chloramphenicol resistance (Cm^r) to produce Campbell insertions interrupting *spmB* and *spmA*, respectively. The correct chromosomal constructs were confirmed by Southern hybridization (40).

To construct an in-frame deletion of *dacB*, pCB1 was treated with *Sty*I, the Klenow fragment of *E. coli* DNA polymerase I, dNTPs, and *Bam*HI to produce a 1,100-bp fragment that was ligated with a 5,500-bp fragment produced by treatment of pCB1 with *Bgl*II, the Klenow fragment of *E. coli* DNA polymerase I, dNTPs, and *Bam*HI. Codons 51 to 105 of *dacB*, including the putative catalytic serine residue (10, 13), were deleted in the resulting plasmid, pDPC221 (Fig. 1). The deletion was verified by DNA sequencing with the primer 5′ GTGAATA CAGCACATGCTGC 3′, which corresponds to positions 653 to 672 in the sequence presented previously (10). To construct an in-frame deletion in *spmA*, pDPC214 was treated with *Hin*fI, the Klenow fragment of *E. coli* DNA polymerase I, dNTPs, and *Eco*RV to produce a 289-bp fragment which was inserted into *Hin*cII-digested pUC19. In the resulting plasmid, pDPC223, the partial *dacB* sequence was in the orientation opposite to that of *lacZ*. The 684-bp *Eco*RV-*Hin*dIII fragment of pDPC211 was then inserted into pDPC223, which had been treated with *Pst*I, T4 DNA polymerase to render the ends blunt, and *Hin*dIII to produce pDPC225. The 880-bp *Bam*HI-*Hin*dIII fragment of pDPC225 was then inserted into *Bam*HI-*Hin*dIII-digested pJH101 to produce pDPC226 (Fig. 1). In pDPC226, codons 15 to 164 of *spmA* were deleted, and a threonine codon (ACC) derived from the pUC19 polylinker was inserted in their place. The deletion was verified by DNA sequencing with the primer 5′ CCGATCAATGA TAATGGCACCG 3′, which corresponds to the complement of positions 2258 to 2279 in the sequence presented previously (10). The two in-frame deletions were moved into the *B. subtilis* chromosome by transformation with pDPC220 and pDPC226 and selection for Cm^r. Campbell-type integration of the plasmids results in the presence of two copies of the gene of interest. The resulting transformants were screened by Southern hybridization (40) for a strain in which both copies of the gene contained the in-frame deletion. Such a strain can result from either a gene conversion event or by recombination between the chromosome and two copies of the transforming plasmid. The desired strains were then grown nonselectively for several generations, plated for single colonies, and screened for chloramphenicol sensitivity (Cm^s) by replica plating. The presence of a single deleted copy of the gene of interest was confirmed by Southern hybridization (40).

***lacZ* fusion constructions.** To construct a translational fusion of *dacB* to *lacZ*, the 177-bp *Sau*3AI fragment of pCB1 was inserted into *Bam*HI-digested pUC19 to produce pDPC224 in which *dacB* and *lacZ* are in opposite orientations. The 200-bp *Sma*I-*Pst*I fragment of pDPC224 was then inserted into *Sma*I-*Pst*I-digested pBluescript IIKS(+) (Stratagene) to produce pDPC228. Finally, the 200-bp *Eco*RI-*Sma*I fragment of pDPC228 was inserted into *Eco*RI-*Sma*I-digested pJF751 (11) to produce pDPC229 (Fig. 1), in which the 11th codon of *dacB* is fused to *lacZ*.

To construct a translational fusion of *spmA* to *lacZ*, pDPC222 (pDPC222 is identical to pDPC223 except that the insert in the *Hin*cII site of pUC19 is in the opposite orientation) was treated with *Hin*dIII, the Klenow fragment of *E. coli* DNA polymerase I, dNTPs, and *Bam*HI. The resulting 280-bp fragment was inserted into pJF751 (11), which had been treated with *Eco*RI, the Klenow fragment of *E. coli* DNA polymerase I, dNTPs, and *Bam*HI to produce pDPC227 (Fig. 1). The 14th codon of *spmA* was fused to *lacZ* in this construct.

To construct a translational fusion of *spmB* to *lacZ*, the 352-bp *Xmn*I-*Eco*RI fragment of pDPC211 was ligated with the 5.4-kb *Sma*I-*Sac*I fragment of pJF751 and the 1.9-kb *Eco*RI-*Sac*I fragment of pJF751 (11) to produce pDPC230 (Fig. 1). In this construct, the 19th codon of *spmB* is fused to *lacZ*.

Each of these three translational fusions was converted to a transcriptional fusion by replacing the 800-bp *Bam*HI-*Cla*I fragment containing the beginning of *lacZ* with the corresponding fragment from pDG268 (2). A 2-bp deletion in this fragment of pDG268 (15, 19) resulted in the absence of a stop codon between our genes of interest and the translation start signals for *lacZ*. We therefore digested each of the three transcriptional fusion plasmids with *Bam*HI, filled the ends with the Klenow fragment of *E. coli* DNA polymerase I and dNTPs, and ligated the DNA. This changed the reading frame such that translation of our genes of interest terminated slightly downstream of the *Bam*HI site and did not interfere with translation initiation of *lacZ*. The plasmids containing the resulting transcriptional fusions to *dacB*, *spmA*, and *spmB* are pDPC234, pDPC235, and pDPC236, respectively (Fig. 1). The nucleotide sequences of all *lacZ* fusion constructs were determined with a Sequenase kit (U.S. Biochemical).

The fusion plasmids were inserted into the corresponding loci on the chromosome by transformation of strains PS832, PS2066, and PS2185 with selection for Cm^r. The antibiotic resistance associated with each insertion was then changed to spectinomycin resistance (Sp^r) by transformation with linearized pJL62 (23). Chromosomal DNA from PS832 carrying the Sp^r-associated fusions was used to transform PS1899 and PS2030 with selection for Sp^r and Cm^r. The presence of all mutations and fusions on the chromosome was verified by Southern hybridization. Chromosomal DNA was purified from a sample of each culture used for measurement of β-galactosidase expression and analyzed to verify that no rearrangement had taken place among the multiple plasmids inserted in the *dacB* region of the chromosome.

Measurement of GPR processing and SASP levels. Various strains carrying plasmid pPS1669 (36), which directs high-level expression of *Bacillus megaterium* GPR in *B. subtilis*, were sporulated in 2× SG medium. At various times, 10-ml samples were harvested for analysis of SASP or P_{46} and P_{41} levels (16), and 2-ml samples were taken for analysis of DPA (30). Samples for analysis of P_{46} and P_{41} were lyophilized and then disrupted and extracted as described previously (16). Aliquots of various samples were subjected to sodium dodecyl sulfate-polyacrylamide gel electrophoresis (SDS-PAGE), proteins were transferred to polyvinylidene difluoride paper, and P_{46} and P_{41} were detected with antiserum against *B. megaterium* GPR as described previously (16). Samples for SASP analysis were also lyophilized, broken, extracted, and dialyzed as described previously, and the three major *B. subtilis* SASP (α, β, and γ) were separated by electrophoresis on polyacrylamide gels run at low pH (16).

Biochemical assays. β-Galactosidase specific activity was assayed with *o*-nitrophenyl-β-D-galactopyranoside or 4-methylumbelliferyl-β-D-galactosidase as described previously (30). The DPA content of spores was assayed as described previously (30). The degree of spore cortex peptidoglycan cross-linking was assayed with fluorodinitrobenzene as described previously (33). The wet density of the spore protoplast was determined by equilibrium density centrifugation on metrizoic acid (Sigma) gradients as described previously (26). Prior to density determination, spores were decoated for 90 min at 37°C in 50 mM Tris-HCl (pH 8.0)–8 M urea–1% (wt/vol) SDS–50 mM dithiothreitol and washed three times with 150 mM NaCl and twice with water. The decoated spores were equilibrated for 60 min in 50% metrizoic acid prior to loading onto gradients.

For determinations of hexosamine and diaminopimelic acid (dpm), spores were decoated and put through two cycles of consecutive extractions with trichloroacetic acid and SDS-dithiothreitol as described previously (33). Extracted spores were then assayed for hexosamine as described previously (14) and for dpm by analysis with a Beckman System 7300 amino acid analyzer. Known amounts of *N*-acetylglucosamine, *N*-acetylmuramic acid, and dpm (Sigma) were assayed in parallel. *N*-Acetylglucosamine and *N*-acetylmuramic acid had identical absorbance coefficients in our assay. Destruction of hexosamine during hydrolysis in the presence of extracted spores was estimated by mixing a known amount of *N*-acetylglucosamine or *N*-acetylmuramic acid with an equivalent amount of each spore sample.

Electron microscopy. Electron micrographs of decoated spores were produced as described previously (37). Micrographs at magnifications of ×18,000 to ×29,000 were measured by hand. The inner boundary of the cortex was defined as the outer edge of the inner spore membrane. The outer boundary of the cortex was defined as the innermost intrusion of the spore coat layers. Protoplast and sporoplast (protoplast-plus-cortex) volumes were calculated as described previously (6).

RESULTS

***dacB* is the first gene in a three-gene operon.** DNA sequence analysis of the *dacB* region of the chromosome has led to the suggestion that *dacB* is the first gene in a three-gene operon (39). We used transcriptional fusions to *lacZ* to demonstrate that *dacB* and the two genes found downstream do indeed form an operon. We propose using the gene designation *spm* (spore maturation) for reasons cited below and naming these two latter genes *spmA* and *spmB* (Fig. 1). Previous data demonstrated that *dacB* is expressed from a single promoter approximately 2 h after the initiation of sporulation (38). β-Galactosidase activity was expressed from a *dacB-lacZ* transcriptional fusion at this same point in sporulation (Fig. 2). Transcriptional fusions of *lacZ* to *spmA* and *spmB* were expressed at the same time and to approximately (within a factor of two) the same level (Fig. 2). An insertion mutation in *dacB* blocked expression of the *spmA*- and *spmB-lacZ* fusions, reducing the β-galactosidase activity to the level found in a strain containing no fusion (data not shown), whereas an in-frame deletion of part of *dacB* had no effect on expression (Fig. 2). The in-frame deletion in *spmA* also had no effect on expression of the *spmB-lacZ* fusion (Fig. 2). These results indicate that transcription of *spmA* and *spmB* originates upstream of *dacB*.

To get some idea of the relative levels of expression of the three proteins encoded by this operon, we repeated the exper-

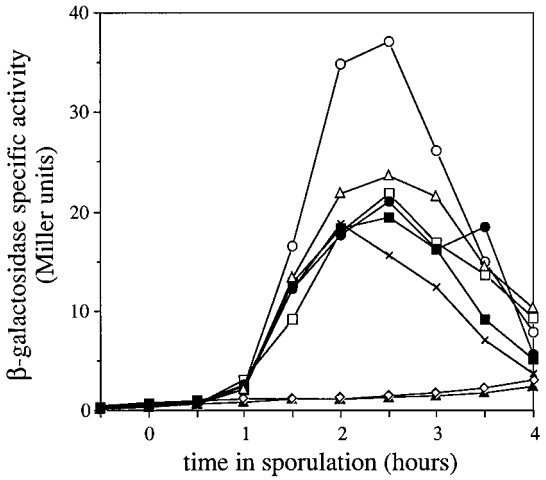

FIG. 2. Expression of transcriptional fusions to *lacZ*. Strains were grown and sporulated in 2× SG medium at 37°C. Time zero is defined as the end of exponential growth and the entry into sporulation. Symbols: □, PS2239, *spmA-lacZ*; ×, PS2240, *dacB-lacZ*; ○, PS2241, *spmB-lacZ*; ■, PS2242, in-frame Δ*dacB spmA-lacZ*; ●, PS2243, in-frame Δ*dacB spmB-lacZ*; △, PS2244, in-frame Δ*spmA spmB-lacZ*; ◇, PS2245, *dacB*::Cm^r *spmA-lacZ*; ▲, PS2246, *dacB*::Cm^r *spmB-lacZ*.

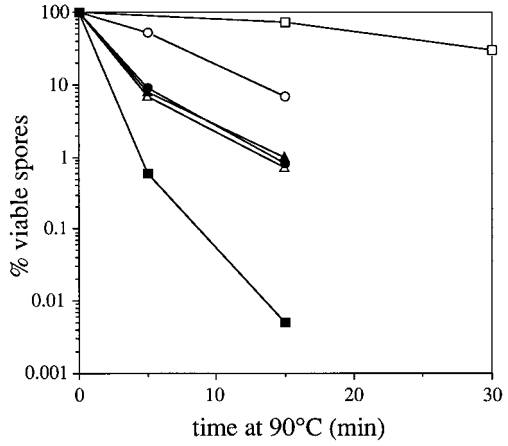

FIG. 3. Heat resistance of purified spores. Spore suspensions were heated at 90°C for the indicated times and then plated to determine viability. Symbols: □, PS832, wild type; ■, PS1899, *dacB*::Cm^r; △, PS2029, *spmB*::Cm^r; ▲, PS2030, *spmA*::Cm^r; ○, PS2066, in-frame Δ*dacB*; ●, PS2185, in-frame Δ*spmA*. The data presented are from one of the three determinations used to calculate the D_{90} values in Table 2; therefore, the values in Table 2 do not agree completely with the apparent D_{90} values shown here.

iments described above with translational fusions to *lacZ*. In each of the three constructs, as little as possible of the gene of interest was fused to *lacZ* to avoid possible problems with membrane association of β-galactosidase. For each fusion, β-galactosidase activity appeared at the same time as that seen with the transcriptional fusions (data not shown). Whereas the transcription levels of all three genes of the operon were approximately equal (Fig. 2), translation of the two distal genes was relatively poor. The maximum β-galactosidase specific activities expressed from the *dacB*-, *spmA*-, and *spmB-lacZ* translational fusions were 98, 4, and 14 Miller units, respectively (data not shown). The specific activity produced by the *spmA-lacZ* fusion was only twofold above the endogenous activity found in a strain lacking a fusion when assayed with *o*-nitrophenyl-β-D-galactopyranoside. This difference was eightfold when assayed with 4-methylumbelliferyl-β-D-galactoside (data not shown). Expression of *spmA*- and *spmB-lacZ* translational fusions was blocked by the *dacB* insertion mutation but not by upstream in-frame deletions (data not shown).

Effects of mutations in *dacB*, *spmA*, and *spmB* on spore resistance properties. To determine if the effect on spore heat resistance previously observed in a *dacB* insertion mutant strain (9) was due to loss of PBP5* or the products of *spmA* or *spmB*, we constructed strains carrying mutations affecting each of the three genes in the *dacB* operon individually. With *dacB*, we constructed an in-frame deletion which removed 55 of the 382 codons (Fig. 1, pDPC221), including the putative active-site serine conserved in all PBPs (10, 13). With *spmA*, we constructed an in-frame deletion removing 149 of the 196 codons (Fig. 1, pDPC226). That these in-frame deletions had no effect on expression of downstream genes is demonstrated by the results of the experiments using the fusions to *lacZ* described above. The mutation affecting *spmB* alone is a Campbell-type insertion which truncates the gene after 100 of its normal 179 codons. In addition, we examined the effects of the original *dacB* insertion mutation which blocks expression of all three genes and of an insertion in *spmA* which blocks expression of both *spmA* and *spmB*. All of these strains sporulated with equal efficiencies, producing approximately 10^9 chloroform-resistant spores per ml. We obtained identical results when we assayed spore heat resistance with chloroform-treated cultures and purified spores (data not shown).

The insertion mutation in *dacB* produced a significant loss of spore heat resistance (Fig. 3 and Table 2, strain PS1899), very similar to that previously observed (9). Mutations affecting any single one of these genes or both *spmA* and *spmB* resulted in the production of spores with an intermediate level of heat resistance (Fig. 3 and Table 2, strains PS2185, PS2029, and PS2030). The strain carrying the in-frame deletion in *dacB* (strain PS2066) was consistently slightly more heat resistant

TABLE 2. Effects of mutations on spore properties

Strain (genotype)	Heat resistance (D_{90} [min])[a]	Amt of DPA per OD_{600} unit (μg)[b]	Protoplast wet density (g/ml)[b]	Mol of hexosamine/ mol of dpm[c]	% dpm cross-linked[c]
PS832 (wild type)	49	14	1.367	4.4	43
PS1899 (*dacB*::Cm^r)	3	17	1.326	2.2	74
PS2066 (in-frame Δ*dacB*)	10	18	1.367	2.8	81
PS2185 (in-frame Δ*spmA*)	6	15	1.345	4.6	50
PS2029 (*spmB*::Cm^r)	7	15	1.346	4.3	44
PS2030 (*spmA*::Cm^r)	7	15	1.347	4.4	42

[a] Values are averages of determinations of three different spore preparations. Variation in these values among experiments was 20 to 40% for a particular strain, but within each experiment, the relative degrees of heat resistance among all strains were the same.
[b] Values are averages of determinations of three different spore preparations. OD_{600}, optical density at 600 nm.
[c] Values presented are averages of determinations of two different spore preparations.

than strains with mutations in *spmA* or *spmB* (Fig. 3 and Table 2). These results indicate that the loss of heat resistance produced by the insertion mutation in *dacB* is due partially to loss of expression of *spmA* and *spmB*.

Effects of *dacB* and *spm* mutations on spore core wet density. Previous studies have indicated a correlation between spore heat resistance and spore protoplast hydration measured as wet density (5, 29). We decoated spores prior to density determination such that the density gradient material could permeate through the cortex (26); the density measured was therefore that of the spore core or protoplast. Interestingly, loss of *dacB* expression alone produced no change in the spore protoplast wet density relative to that of the wild-type strain (Table 2, strain PS2066). Mutations affecting *spmA*, *spmB*, or both produced a significant reduction in the spore protoplast wet density (Table 2, strains PS2185, PS2029, and PS2030). The insertion mutation in *dacB* produced the most dramatic reduction in protoplast wet density (Table 2, strain PS1899). On the basis of previous work (26), these wet densities translate to spore protoplast water contents (in grams of H_2O per gram [dry weight]) of approximately 0.59 for the wild type, 0.79 for *spmA* and *spmB* mutants, and 1.08 for the *dacB* insertion mutant.

DPA contents of mutant spores. Some evidence suggests that accumulation and maintenance of DPA in the spore is required for development of heat resistance (4). We wished to determine if a DPA deficit might be responsible for the heat sensitivity of our mutant spores. However, the amount of DPA contained in the spores of our wild-type and mutant strains was relatively constant (Table 2). We also verified that the decoating procedure removed little if any DPA from the spores of each strain (≤15% of total DPA in all cases). The spore core wet density differences observed are, therefore, apparently not due to losses of spore contents during decoating. We did find that heating of *dacB* and *spmA* mutant spores at 70°C resulted in significant losses of DPA. After 45 min at 70°C, the wild-type, *dacB* deletion mutant, *spmA* deletion mutant, and *dacB* insertion mutant spores had lost 11, 24, 33, and 51% of their DPA, respectively. This same heating resulted in killing of 29, 72, 86, and 92% of the spores of these strains, respectively. At least in the case of the *dacB* deletion mutant spores, this loss of DPA was also accompanied by a significant decrease in the spore protoplast wet density (data not shown). Some loss of DPA from spores upon sublethal heating has been observed previously (7, 20), generally in the range of what we observed with our wild-type strain.

Effects of increased spore core hydration on GPR processing and SASP content. The striking effects of mutations in the *dacB* and *spm* genes on spore heat resistance, presumably due in large part to effects on spore water content, suggested that other sporulation or spore parameters influenced by core water content might be affected by mutations in these genes. One such additional parameter is the timing during sporulation of the processing of the SASP-specific protease GPR from the zymogen form (P_{46}) to the active form (P_{41}) (36). This event normally takes place at about the time of final forespore dehydration and in vitro is greatly stimulated by dehydration (17, 36). Strikingly, the conversion of P_{46} to P_{41} was 45 to 60 min slower relative to DPA accumulation during sporulation of the *dacB* insertion mutant than during sporulation of the wild-type strain (Fig. 4). However, the final levels of GPR processing (~50%) were the same in both strains. A similar delay in P_{46} processing was observed in the *spmA* deletion mutant but not in the *dacB* deletion mutant (data not shown).

Analysis of the SASP accumulated in these strains showed that as found previously (36), overproduction of GPR in the wild-type strain resulted in a significant decrease in the SASP-γ accumulated in spores, with a slight decrease in SASP-β (Fig. 5, lanes 1 to 3). The apparent lower levels of SASP at 9 h (versus 24 h) are in part an artifact of the extraction procedure; extraction from free spores (at 24 h) is more efficient than extraction from sporulating cells (at 9 h). Although the *dacB* insertion mutant did synthesize SASP-γ, this protein was subsequently completely degraded by the time the mutant spore was released from the sporangium; there was also a significant loss of SASP-β (Fig. 5, lanes 4 and 5). Once the spores had been released from the sporangium, there was no further change in SASP levels in *dacB* insertion spores for at least 2 weeks (data not shown). The decreases in SASP-β and -γ in these experiments were not seen with the *dacB* insertion mutant without pPS1669 (data not shown), presumably because

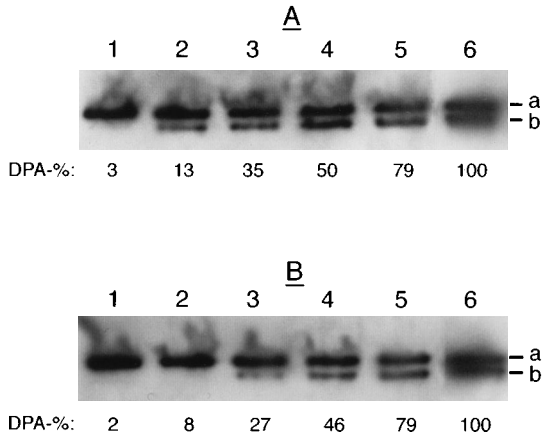

FIG. 4. Processing of P_{46} and P_{41} during sporulation of wild-type (A) and *dacB* insertion (B) strains. *B. subtilis* PS1669 (wild type with pPS1669) and PS2198 (*dacB* insertion with pPS1669) were grown and sporulated in 2× SG medium, and samples were taken and GPR and DPA were extracted as described in Materials and Methods. Aliquots (5 μl of a 1/100 dilution) of GPR extracts were subjected to SDS-PAGE, protein was transferred to polyvinylidene difluoride paper, and P_{46} and P_{41} were detected with a 1/10,000 dilution of anti-GPR as described in Materials and Methods. The samples in panel A, lanes 1 to 6, were harvested at 4, 5, 6, 7, 8, and 24 h of sporulation, respectively; those in panel B, lanes 1 to 6, were harvested at 4, 5, 6, 7, 9, and 24 h of sporulation, respectively. The horizontal bars labeled a and b denote the migration positions of P_{46} and P_{41}, respectively. The values below the lanes give the percentages of maximum DPA accumulated by the cultures at these points in sporulation.

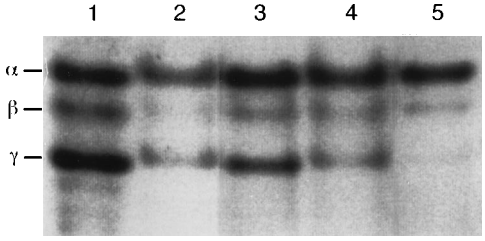

FIG. 5. SASP level late in sporulation of wild-type and *dacB* insertion strains expressing high levels of GPR. *B. subtilis* PS1669 (wild type) and PS2198 (*dacB* insertion) carrying plasmid pPS1669 expressing high GPR levels as well as PS832 (wild type) were grown and sporulated in 2× SG medium, and samples were taken, extracted, and subjected to acrylamide gel electrophoresis at a low pH to resolve the major SASP. Lanes: 1, PS832 harvested at 24 h of sporulation; 2, PS1669 harvested at 9 h of sporulation; 3, PS1669 harvested at 24 h of sporulation; 4, PS2198 harvested at 9 h of sporulation; 5, PS2198 harvested at 24 h of sporulation. The horizontal lines adjacent to lane 1 denote the migration positions of SASP-α, -β, and -γ.

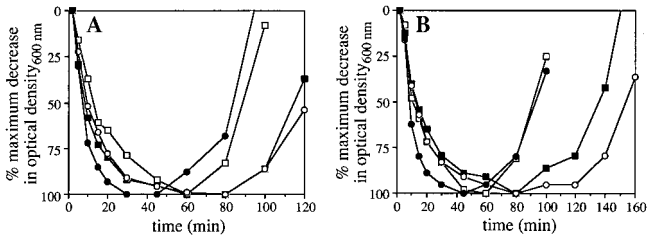

FIG. 6. Spore germination and outgrowth in the presence and absence of heat activation. The optical density of a purified spore suspension was determined at the times indicated following inoculation into 2× YT medium containing 4 mM L-alanine at 37°C. The experiment was performed without (A) or with (B) a 15-min spore activation at 70°C prior to inoculation. Symbols: □, PS832, wild type; ■, PS1899, *dacB*::Cm^r; ○, PS2066, in-frame Δ*dacB*; ●, PS2185, in-frame Δ*spmA*. The optical density is presented as a percentage of the maximum decrease observed for each individual strain during the experiment to account for differences in this value among the strains. We attribute these differences to small numbers (<10%) of germinated spores in some of the preparations and killing of spores during heat activation. The maximum percentages of decrease in optical density at 600 nm in the absence of heat activation were 43, 48, 44, and 52% for PS832, PS1899, PS2066, and PS2185, respectively. The maximum percentages of decrease following heat activation were 50, 32, 40, and 40%, respectively.

this plasmid increases the level of active GPR 200- to 500-fold over that in wild-type spores (36).

Germination and outgrowth of mutant spores. Mutations affecting *spmA*, *spmB*, and *dacB* also produced slight changes in kinetics of spore germination and outgrowth. The spores of the *spmA* in-frame deletion strain did not require heat activation to achieve the maximum germination rate (Fig. 6A). The optical density of a suspension of spores of this strain decreased faster than that of the wild-type strain upon exposure to germinants (Fig. 6A). This was also true for spores produced by strains containing insertion mutations in *spmA* and *spmB* (data not shown). Following heat activation at 70°C for 15 min, germination and outgrowth of the wild-type and the *spmA* deletion spores appeared similar (Fig. 6B); however, the total percent decrease in optical density of the *spmA* mutant spores was less than that observed prior to activation. This may be due to loss of DPA or other spore contents and some spore killing. Germination of spores produced by strains carrying an insertion or an in-frame deletion in *dacB* was similar to that of wild-type spores (Fig. 6). The requirement for heat activation was difficult to assess with these spores as a result of losses of optical density and a significant degree of killing upon heating. Relative to the wild type, there was a reproducible 20- to 30-min delay in the outgrowth of *dacB* mutant spores in the absence of heat activation (Fig. 6A). The apparent increase in this delay following heat activation (Fig. 6B) could be attributed to heat killing.

Cortex peptidoglycan structural changes in *dacB* mutants. Loss of PBP5*, a D,D-carboxypeptidase, might be expected to alter the degree of peptide cross-linking of the cortex peptidoglycan, because cleavage of D-alanine from peptide side chains by this enzyme renders them unable to serve as donors in D-alanine–dpm cross-link formation. When we examined this aspect of cortex structure in the spores of all of our strains, we found that relative to the wild type, almost twice as much of the dpm was in cross-links in strains carrying *dacB* mutations (Table 2, strains PS1899 and PS2066). In contrast, mutations affecting *spmA*, *spmB*, or both had no significant effect on the degree of cortex cross-linking (Table 2, strains PS2185, PS2029, and PS2030). In the course of these analyses of levels of cortex cross-linking, we noticed that the amount of dpm per unit of spores appeared to be consistently higher in strains carrying *dacB* mutations. We therefore assayed the amount of dpm relative to the amount of hexosamine present in the various spore preparations. The amounts of hexosamine per unit of spores were very similar in all of the strains (data not shown), indicating that the cortex contents of the spores were not changed. The ratio of dpm to hexosamine in strains carrying mutations affecting *spmA*, *spmB*, or both was identical to that found for the wild type (Table 2, strains PS2185, PS2029, and PS2030). However, strains carrying *dacB* mutations produced spores containing approximately twice as much dpm per unit of hexosamine, relative to the wild type (Table 2, strains PS1899 and PS2066).

Electron microscopy of spores. We prepared electron micrographs of our spore preparations to determine whether the changes in cortex structure and core wet density that we observed resulted in visible changes in the spore's appearance. Indeed, mutations affecting *dacB* and *spmA* resulted in significant changes in the appearance of spore thin sections. In wild-type spores, the area corresponding to the cortex contained no discernible structure (Fig. 7A). However, in the spores produced by the strain carrying an insertion mutation in *dacB*, a well-defined cortex was visible (Fig. 7B), although in many spores the cortex did not appear to fill the entire space between the core and the coat structure. Loss of *dacB* alone resulted in the cortex having a similarly well-defined appearance (Fig. 7C). The strain carrying the in-frame deletion of *spmA* produced a spore cortex with an intermediate appearance. Some structure was visible in the space between the core and coats, but its boundaries were generally less well defined (Fig. 7D).

Previous studies used measurements of electron micrographs of centrally longitudinal thin sections of spores to reveal a correlation between spore heat resistance and the ratio of the spore protoplast volume to the sporoplast (protoplast-plus-cortex) volume (6). We used this same technique to make estimates of spore protoplast and sporoplast volumes in our wild-type and mutant spores. The ratio of protoplast volume to sporoplast volume in wild-type spores was 0.254 ± 0.074 (n = 18). This ratio increased significantly in spores produced by strains carrying mutations in *dacB* or *spmA*. For the *dacB* insertion and deletion strains, we calculated ratios of 0.412 ± 0.054 (n = 14) and 0.488 ± 0.063 (n = 13), respectively. Spores produced by the *spmA* deletion strain had a protoplast-to-sporoplast volume ratio of 0.427 ± 0.066 (n = 17).

Effects of mutations eliminating other PBPs. Observation of spore cortex structural changes and a reduction in heat resistance associated with loss of PBP5* led us to examine these and other characteristics of spores produced by strains lacking other PBPs, especially those demonstrated or predicted to be D,D-carboxypeptidases (PBP5 [8] and the *dacF* product [48]) and those induced during sporulation (PBP4* [41] and PBP2c [35]). (We were unable to examine *spoVD* mutant spores because these strains do not produce stable spores.) As had been found previously, we detected no change in spore heat resistance associated with mutations affecting *dacA* (PBP5) (9), *dacF* (putative PBP) (48), *pbpE* (PBP4*) (34), or *pbpF* (PBP2c) (35). We also found no significant difference between these spores and those of the wild type when we assayed DPA, hexosamine, and dpm content, degree of peptidoglycan cross-linking, spore core wet density, and germination kinetics.

DISCUSSION

We have demonstrated that *dacB* is the first gene in a three-gene operon. Expression of this operon appears to originate uniquely at the previously defined σ^E-dependent promoter up-

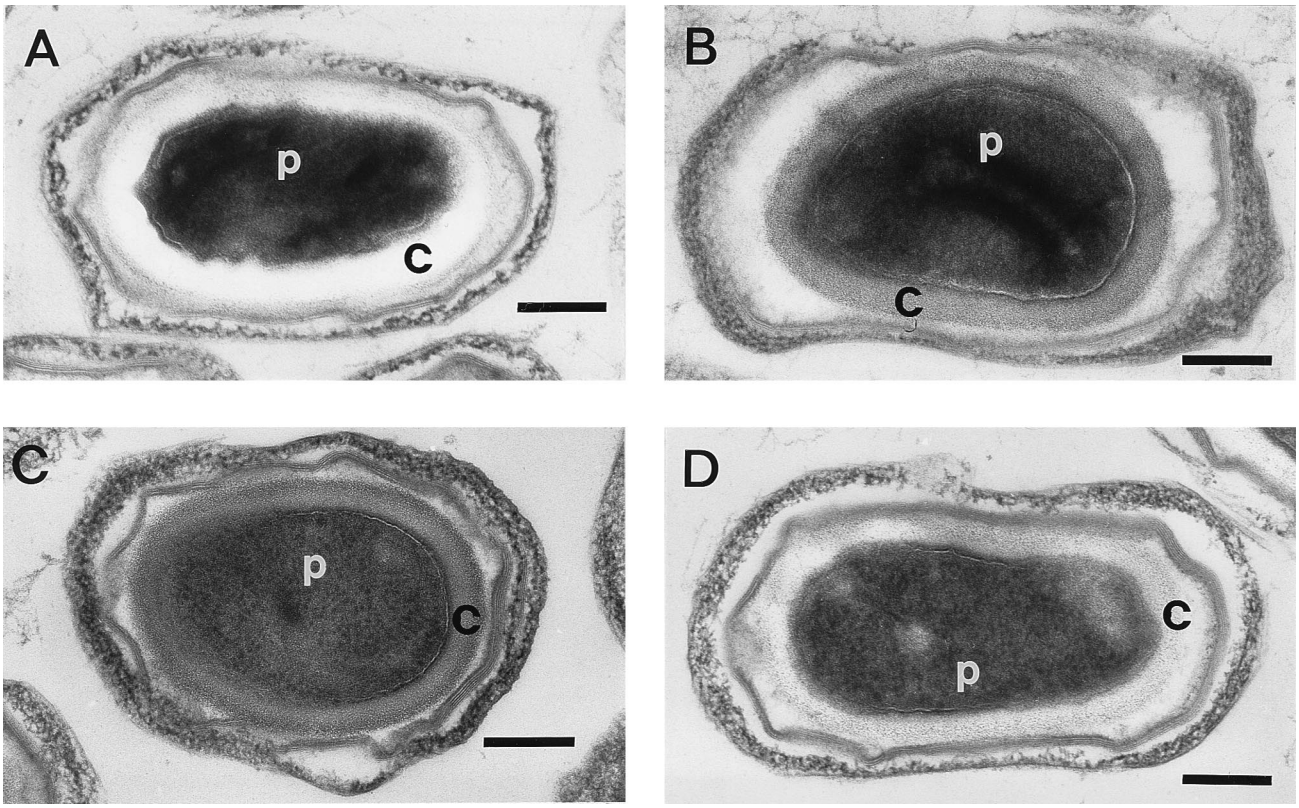

FIG. 7. Transmission electron micrographs of wild-type, *dacB* mutant, and *spm* mutant spores. Purified, decoated spores were fixed, embedded, and sectioned as described in Materials and Methods. (A) PS832, wild type; (B) PS1899, *dacB*::Cm^r; (C) PS2066, in-frame Δ*dacB*; (D) PS2185, in-frame Δ*spmA*. The amount of space between the well-defined cortex structure and the coat layers in the *dacB* mutant spores was highly variable. Bars, 0.2 μm. p, protoplast or core; c, cortex.

stream of *dacB* (38). The second and third genes, *spmA* and *spmB*, appear to be poorly translated, presumably because of a poor potential ribosome binding site upstream of *spmA* and a 10-base overlap in the *dacB* and *spmA* coding sequences (39). We note that the poor translation of *spmA* and *spmB* we observed may lead to general instability of the *dacB* operon message; whereas the 5′ end of the message has been detected by primer extension (38), an attempt to detect the full-length message by Northern (RNA) hybridization was unsuccessful (3). An insertion mutation in *dacB* was shown previously to result in the production of spores with reduced heat resistance (9). Our data demonstrate that this loss of heat resistance is partially due to a lack of expression of *spmA* and *spmB*.

Analysis of the peptidoglycan structure in the cortex of the *dacB* (either insertion or deletion) mutant spores revealed that peptide side chains are attached to 71 to 91% of the muramic acid residues, compared with 45% in the wild type. Previous results indicated that peptides were attached to 35% of the muramic acid residues in the wild-type cortex and that an additional 50% of the muramic acid was converted to muramic acid lactam and thus had no side chain (46, 47). It would appear that the *dacB* mutant spores contain little, if any, muramic acid lactam, although further experiments are needed to verify this. In addition, 78% of the dpm in the *dacB* mutant cortex was involved in peptide cross-link formation, compared with 43% in the wild type. The D,D-carboxypeptidase activity associated with PBP5* (43), the *dacB* product, might be expected to have a role in regulation of the degree of cross-linking, since removal of the terminal D-alanine of a peptide side chain results in the inability of this peptide to function as a donor in D-alanine–dpm cross-link formation. The 70 to 80% level of cross-linking found in the *dacB* mutant spore cortex is at the theoretical limit for cross-linking in a multilayered peptidoglycan structure containing this type of peptide side chain (22). This suggests that PBP5* may be the major, and possibly the only, factor involved in regulating the degree of cortex peptide cross-linking. However, modification of the cortex glycan chains may alter the predicted maximum degree of cross-linking (22). We speculate that cleavage by PBP5* of one or both of the terminal D-alanines from the original pentapeptide creates a substrate for subsequent removal of more of the peptide, a process which could lead ultimately to muramic acid lactam formation (42). The slow outgrowth of *dacB* mutant spores might be due to resistance of the altered cortex to degradation by the normal cortex lytic enzymes. Enzymes involved in normal vegetative wall expansion could eventually allow outgrowth of these cells.

Theories suggesting that a mechanical activity of the spore cortex might be involved in attaining dehydration of the spore core (25, 45) have incorporated the ability of a loosely cross-linked peptidoglycan to expand and contract in response to changes in ionic strength (12, 31). The fact that the spores produced by our *dacB* deletion strain exhibit normal dehydration refutes these theories. An earlier suggestion that the cortex is merely a very highly cross-linked retaining wall involved in maintaining core dehydration (27) would also appear to be incorrect. The highly cross-linked *dacB* mutant cortex should be an effective retaining wall, yet the loosely cross-linked wild-type cortex is more effective at maintaining heat resistance. Spore heat resistance has been found previously to correlate

with a number of spore characteristics, including the amount of cortex peptidoglycan (18), the ratio of spore protoplast (core) volume to sporoplast (core-plus-cortex) volume (6), and the spore core wet density (5, 29). We found no significant difference in the amounts of peptidoglycan per unit of spores among our strains, but measurements of electron micrographs indicated that there was a significant increase in the protoplast/sporoplast volume ratios in *dacB* insertion, *dacB* deletion, and *spm* mutant spores. Interestingly, this ratio change was found in both the presence (*spm* mutants) and absence (*dacB* deletion) of a change in spore core hydration. It is tempting to speculate that this increased ratio in the *dacB* and *spm* mutants is due to an alteration in cortex structure, resulting in a shift from an extended to a compact peptidoglycan conformation. However, the degree of variation in our measurements does not allow us to state whether the ratio changes are due to an increase in protoplast volume, a decrease in cortex volume, or both. In addition, the potential for artifactual variation in spore component volume upon preparation for electron microscopy makes extrapolation of these data to the situation in viable, hydrated spores questionable.

Gerhardt and colleagues have demonstrated that heat resistance is correlated with core wet density in spores produced by a variety of species and under differing growth conditions (5, 29). We have now demonstrated a similar qualitative correlation with isogenic spores whose cores appear to differ only in their water contents. However, the wild-type protoplast wet density of the spores produced by the *dacB* deletion strain did not correlate with their lowered heat resistance, indicating that cortex structure is one additional factor involved in maintaining heat resistance. This effect may be due to leakage of DPA and other core solutes from the *dacB* deletion mutant spores upon heating, which results in a decreased protoplast wet density. Indeed, when wild-type and *dacB* mutant spores are dried, they exhibit identical levels of heat resistance (32), suggesting that a defective cortex results in heat sensitivity only when influx of water into the spore is possible.

At approximately the time of final spore dehydration, 50% of the spore protease (GPR) is processed from its zymogen form (P_{46}) to its active form (P_{41}) (36). In vitro processing of P_{46} is also greatly stimulated by dehydration (17). When GPR is greatly overproduced during sporulation in a wild-type strain, 50% of the protease is still processed to P_{41} at the normal time, and this higher level of P_{41} appears to result in degradation of a significant portion of the SASP-γ and a small amount of SASP-β (36). When GPR overproduction is carried out in the *dacB* insertion or *spmA* deletion mutants, processing of the protease takes place with much slower kinetics and 50% processing is achieved at a significantly later time during sporulation. These data are consistent with a slower dehydration of the spore protoplast in *dacB* insertion and *spmA* deletion mutants than in the wild-type strains. SASP-γ was synthesized in the *dacB* insertion mutant but, in the presence of increased amounts of P_{41}, was subsequently degraded completely; a significant amount of SASP-β was also lost. These data suggest that P_{41} formed in the *dacB* insertion mutant may be able to act on SASP more readily than P_{41} formed in wild-type spores, possibly because there may be a slightly higher spore core water content at the time of P_{41} generation in the *dacB* spores.

Mutations affecting the *spm* genes resulted in the production of spores with reduced core wet density. Delayed GPR processing in an *spmA* deletion strain suggests that the defect in these spores is an inability to attain normal protoplast dehydration as opposed to an inability to maintain dehydration. The roles of the *spm* gene products in spore core dehydration are unknown, but we can speculate on two possibilities. First, these proteins might be involved in transport of something into or out of the forespore. The predicted products of *spmA* and *spmB* have four to five and two highly hydrophobic regions, respectively, which might function as membrane interaction or membrane-spanning regions. Second, these proteins might be required, directly or indirectly, for some modification of the cortex peptidoglycan structure. Although we detected no change in the *spm* mutant cortex chemical structure, a more detailed analysis might do so. A more subtle change in cortex structure could be a change in the three-dimensional structure of the peptidoglycan lattice in the absence of a chemical modification. None of these possible mechanisms of *spm* product action are exclusive; modification of the forespore ionic environment via transport could bring about a change in cortex conformation, which could then lead to a further chemical modification. Determination of the location of these proteins in the sporangium (i.e., mother cell cytoplasm, cortical space, spore core, or mother cell, outer forespore, or inner forespore membranes) and in vitro analysis of their activities will be interesting future studies. A more detailed examination of wild-type, *dacB* mutant, and *spm* mutant cortex structures during synthesis, dormancy, and germination will further expand our understanding of the role of this structure in spore core dehydration and spore heat resistance.

ACKNOWLEDGMENTS

We thank Christine Buchanan, Pat Piggot, and David Ellar for providing strains, Arthur Hand for electron microscopy, and George Korza for performing amino acid analyses.

This work was supported by grant GM19698 from the National Institutes of Health.

REFERENCES

1. **Anagnostopoulos, C., and J. Spizizen.** 1961. Requirements for transformation in *Bacillus subtilis*. J. Bacteriol. **81:**74–76.
2. **Antoniewski, C., B. Savelli, and P. Stragier.** 1990. The *spoIIJ* gene, which regulates early developmental steps in *Bacillus subtilis*, belongs to a class of environmentally responsive genes. J. Bacteriol. **172:**86–93.
3. **Azevedo, V., A. Sorokin, S. D. Ehrlich, and P. Serror.** 1993. The transcriptional organization of the *Bacillus subtilis* 168 chromosome region between the *spoVAF* and *serA* genetic loci. Mol. Microbiol. **10:**397–405.
4. **Balassa, G., P. Milhaud, E. Raulet, M. T. Silva, and J. C. F. Sousa.** 1979. A *Bacillus subtilis* mutant requiring dipicolinic acid for the development of heat-resistant spores. J. Gen. Microbiol. **110:**365–379.
5. **Beaman, T. C., and P. Gerhardt.** 1986. Heat resistance of bacterial spores correlated with protoplast dehydration, mineralization, and thermal adaptation. Appl. Environ. Microbiol. **52:**1242–1246.
6. **Beaman, T. C., J. T. Greenamyre, T. R. Corner, H. S. Pankratz, and P. Gerhardt.** 1982. Bacterial spore heat resistance correlated with water content, wet density, and protoplast/sporoplast volume ratio. J. Bacteriol. **150:** 870–877.
7. **Beaman, T. C., H. S. Pankratz, and P. Gerhardt.** 1988. Heat shock affects permeability and resistance of *Bacillus stearothermophilus* spores. Appl. Environ. Microbiol. **54:**2515–2520.
8. **Blumberg, P. M., and J. L. Strominger.** 1972. Five penicillin-binding components occur in *Bacillus subtilis* membranes. J. Biol. Chem. **247:**8107–8113.
9. **Buchanan, C. E., and A. Gustafson.** 1992. Mutagenesis and mapping of the gene for a sporulation-specific penicillin-binding protein in *Bacillus subtilis*. J. Bacteriol. **174:**5430–5435.
10. **Buchanan, C. E., and M.-L. Ling.** 1992. Isolation and sequence analysis of *dacB*, which encodes a sporulation-specific penicillin-binding protein in *Bacillus subtilis*. J. Bacteriol. **174:**1717–1725.
11. **Ferrari, E., S. M. Howard, and J. A. Hoch.** 1985. Effect of sporulation mutations on subtilisin expression, assayed using a subtilisin-β-galactosidase gene fusion, p. 180–184. *In* J. A. Hoch and P. Setlow (ed.), Molecular biology of microbial differentiation. American Society for Microbiology, Washington, D.C.
12. **Gerhardt, P., and R. E. Marquis.** 1989. Spore thermoresistance mechanisms, p. 43–63. *In* I. Smith, R. A. Slepecky, and P. Setlow (ed.), Regulation of prokaryotic development. American Society for Microbiology, Washington, D.C.
13. **Ghuysen, J.-M.** 1991. Serine β-lactamases and penicillin-binding proteins. Annu. Rev. Microbiol. **45:**37–67.
14. **Ghuysen, J.-M., D. J. Tipper, and J. L. Strominger.** 1966. Enzymes that

degrade bacterial cell walls. Methods Enzymol. **8:**685–699.
15. **Gonzy-Tréboul, G., C. Karmazyn-Campelli, and P. Stragier.** 1992. Developmental regulation of transcription of the *Bacillus subtilis ftsAZ* operon. J. Mol. Biol. **224:**967–979.
16. **Illades-Aguiar, B., and P. Setlow.** 1994. Studies of the protease which initiates degradation of small, acid-soluble proteins during germination of spores of *Bacillus* species. J. Bacteriol. **176:**2788–2795.
17. **Illades-Aguiar, B., and P. Setlow.** 1994. Autoprocessing of the protease that degrades small, acid-soluble proteins of spores of *Bacillus* species is triggered by low pH, dehydration, and dipicolinic acid. J. Bacteriol. **176:**7032–7037.
18. **Imae, Y., and J. L. Strominger.** 1976. Relationship between cortex content and properties of *Bacillus sphaericus* spores. J. Bacteriol. **126:**907–913.
19. **Jacob, S., R. Allmansberger, D. Gärtner, and W. Hillen.** 1991. Catabolite repression of the operon for xylose utilization from *Bacillus subtilis* W23 is mediated at the level of transcription and depends on a cis site in the *xylA* reading frame. Mol. Gen. Genet. **229:**189–196.
20. **Keynan, A., and Z. Evenchik.** 1969. Activation, p. 359–396. *In* G. W. Gould and A. Hurst (ed.), The bacterial spore. Academic Press Ltd., London.
21. **Koshikawa, T., T. C. Beaman, H. S. Pankratz, S. Nakashio, T. R. Corner, and P. Gerhardt.** 1984. Resistance, germination, and permeability correlates of *Bacillus megaterium* spores successively divested of integument layers. J. Bacteriol. **159:**624–632.
22. **Labischinski, H., G. Barnickel, D. Naumann, and P. Keller.** 1985. Conformational and topological aspects of the three-dimensional architecture of bacterial peptidoglycan. Ann. Inst. Pasteur Microbiol. **136A:**45–50.
23. **LeDeaux, J. R., and A. D. Grossman.** 1995. Isolation and characterization of *kinC*, a gene that encodes a sensor kinase homologous to the sporulation sensor kinases KinA and KinB in *Bacillus subtilis*. J. Bacteriol. **177:**166–175.
24. **Leighton, T. J., and R. H. Doi.** 1971. The stability of messenger ribonucleic acid during sporulation in *Bacillus subtilis*. J. Biol. Chem. **254:**3189–3195.
25. **Lewis, J. C., N. S. Snell, and H. K. Burr.** 1960. Water permeability of bacterial spores and the concept of a contractile cortex. Science **132:**544–545.
26. **Lindsay, J. A., T. C. Beaman, and P. Gerhardt.** 1985. Protoplast water content of bacterial spores determined by buoyant density sedimentation. J. Bacteriol. **163:**735–737.
27. **Marquis, R. E., and G. R. Bender.** 1990. Compact structure of cortical peptidoglycans from bacterial spores. Can. J. Microbiol. **36:**426–429.
28. **Mason, J. M., and P. Setlow.** 1986. Essential role of small, acid-soluble spore proteins in resistance of *Bacillus subtilis* spores to UV light. J. Bacteriol. **167:**174–178.
29. **Nakashio, S., and P. Gerhardt.** 1985. Protoplast dehydration correlated with heat resistance of bacterial spores. J. Bacteriol. **162:**571–578.
30. **Nicholson, W. L., and P. Setlow.** 1990. Sporulation, germination, and outgrowth, p. 391–450. *In* C. R. Harwood and S. M. Cutting (ed.), Molecular methods for bacillus. John Wiley & Sons Ltd., Chichester, England.
31. **Ou, L.-T., and R. E. Marquis.** 1970. Electromechanical interactions in cell walls of gram-positive cocci. J. Bacteriol. **101:**92–101.
32. **Popham, D. L., S. Sengupta, and P. Setlow.** Unpublished data.
33. **Popham, D. L., and P. Setlow.** 1993. The cortical peptidoglycan from spores of *Bacillus megaterium* and *Bacillus subtilis* is not highly cross-linked. J. Bacteriol. **175:**2767–2769.
34. **Popham, D. L., and P. Setlow.** 1993. Cloning, nucleotide sequence, and regulation of the *Bacillus subtilis pbpE* operon, which codes for penicillin-binding protein 4* and an apparent amino acid racemase. J. Bacteriol. **175:**2917–2925.
35. **Popham, D. L., and P. Setlow.** 1993. Cloning, nucleotide sequence, and regulation of the *Bacillus subtilis pbpF* gene, which codes for a putative class A high-molecular-weight penicillin-binding protein. J. Bacteriol. **175:**4870–4876.
36. **Sanchez-Salas, J. L., and P. Setlow.** 1993. Proteolytic processing of the protease which initiates degradation of small acid-soluble proteins during germination of *Bacillus subtilis* spores. J. Bacteriol. **175:**2568–2577.
37. **Setlow, B., A. R. Hand, and P. Setlow.** 1991. Synthesis of a *Bacillus subtilis* small, acid-soluble protein in *Escherichia coli* causes cell DNA to assume some characteristics of spore DNA. J. Bacteriol. **173:**1642–1653.
38. **Simpson, E. B., T. W. Hancock, and C. E. Buchanan.** 1994. Transcriptional control of *dacB*, which encodes a major sporulation-specific penicillin-binding protein. J. Bacteriol. **176:**7767–7769.
39. **Sorokin, A., E. Zumstein, V. Azevedo, S. D. Ehrlich, and P. Serror.** 1993. The organization of the *Bacillus subtilis* 168 chromosome region between the *spoVA* and *serA* genetic loci, based on sequence data. Mol. Microbiol. **10:**385–395.
40. **Southern, E. M.** 1975. Detection of specific sequences among DNA fragments separated by gel electrophoresis. J. Mol. Biol. **98:**503–517.
41. **Sowell, M. O., and C. E. Buchanan.** 1983. Changes in penicillin-binding proteins during sporulation of *Bacillus subtilis*. J. Bacteriol. **153:**1331–1337.
42. **Tipper, D. J., and J. J. Gauthier.** 1972. Structure of the bacterial endospore, p. 3–12. *In* H. O. Halvorson, R. Hanson, and L. L. Campbell (ed.), Spores V. American Society for Microbiology, Washington, D.C.
43. **Todd, J. A., E. J. Bone, and D. J. Ellar.** 1985. The sporulation-specific penicillin-binding protein 5a from *Bacillus subtilis* is a DD-carboxypeptidase *in vitro*. Biochem. J. **230:**825–828.
44. **Todd, J. A., E. J. Bone, P. J. Piggot, and D. J. Ellar.** 1983. Differential expression of penicillin-binding protein structural genes during *Bacillus subtilis* sporulation. FEMS Microbiol. Lett. **18:**197–202.
45. **Warth, A. D.** 1985. Mechanisms of heat resistance, p. 209–225. *In* G. J. Dring, D. J. Ellar, and G. W. Gould (ed.), Fundamental and applied aspects of bacterial spores. Academic Press Ltd., London.
46. **Warth, A. D., and J. L. Strominger.** 1969. Structure of the peptidoglycan of bacterial spores: occurrence of the lactam of muramic acid. Proc. Natl. Acad. Sci. USA **64:**528–535.
47. **Warth, A. D., and J. L. Strominger.** 1972. Structure of the peptidoglycan from spores of *Bacillus subtilis*. Biochemistry **11:**1389–1396.
48. **Wu, J.-J., R. Schuch, and P. J. Piggot.** 1992. Characterization of a *Bacillus subtilis* sporulation operon that includes genes for an RNA polymerase σ factor and for a putative DD-carboxypeptidase. J. Bacteriol. **174:**4885–4892.